PHYSICAL REVIEW B **79**, 161407(R) (2009)

Tuning the Josephson current in carbon nanotubes with the Kondo effect

A. Eichler,[1] R. Deblock,[2] M. Weiss,[1] C. Karrasch,[3] V. Meden,[3] C. Schönenberger,[1] and H. Bouchiat[2]
[1]*Department of Physics, University of Basel, Klingelbergstrasse 82, CH-4056 Basel, Switzerland*
[2]*Laboratoire de Physique des Solides, CNRS, UMR 8502, Université Paris-Sud, F-91405 Orsay Cedex, France*
[3]*Institut für Theoretische Physik A and JARA—Fundamentals of Future Information Technology, RWTH Aachen University, 52056 Aachen, Germany*

(Received 10 March 2009; published 28 April 2009)

We investigate the Josephson current in a single wall carbon nanotube connected to superconducting electrodes. We focus on the parameter regime in which transport is dominated by Kondo physics. A sizeable supercurrent is observed for odd number of electrons on the nanotube when the Kondo temperature T_K is sufficiently large compared to the superconducting gap. On the other hand when, in the center of the Kondo ridge, T_K is slightly smaller than the superconducting gap, the supercurrent is found to be extremely sensitive to the gate voltage V_{BG}. Whereas it is largely suppressed at the center of the ridge, it shows a sharp increase at a finite value of V_{BG}. This increase can be attributed to a doublet-singlet transition of the spin state of the nanotube island leading to a π shift in the current phase relation. This transition is very sensitive to the asymmetry of the contacts and is in good agreement with theoretical predictions.

DOI: 10.1103/PhysRevB.79.161407 PACS number(s): 72.15.Qm, 73.21.−b, 73.63.Fg, 74.50.+r

Metallic single wall carbon nanotubes (SWNTs) have attracted a lot of interest as one-dimensional (1D) quantum wires combining a low carrier density and a high mobility. Depending on the transparency of the interface between the nanotube and the electrode, the conduction ranges from insulating behavior and strong Coulomb blockade at low transparency to nearly ballistic transport with conductance close to $4e^2/h$ when the transparency is high.[1,2] The intermediate conduction regime is particularly interesting because in the case of an odd number of electrons on the nanotube a strongly correlated Kondo resonant state can form, where the magnetic moment of the unpaired spin is screened by the spins of the electrons in the leads.[3] Moreover, when the carbon nanotubes (CNTs) are in good contact with superconducting electrodes, it is possible to induce superconductivity and observe supercurrents, as was first investigated in ungated suspended devices.[4,5] Proximity induced superconductivity was then explored in gated devices with evidence of a strong modulation of subgap conductance, but in most cases no supercurrent was observed.[6–9] More recently, tunable supercurrents could be detected in the resonant tunneling conduction regime, where the transmission of the contacts approaches unity.[10,11] In this regime, the discrete spectrum of the nanotube is still preserved and the maximum value of supercurrent is observed when the Fermi energy of the electrodes is at resonance with "the electron in a box states" of the nanotube. A superconducting interference device was fabricated with carbon nanotubes as weak links: supercurrent π phase shifts occurred when the number of electrons in the nanotube dot was changed from odd to even[12] corresponding to the transition from a magnetic to a nonmagnetic state. Sharp discontinuities in the critical current at this $0-\pi$ transition in relation with the even-odd occupation number of the nanotube quantum dot were also observed in single nanotube junction devices.[13] As pointed out in the superconducting quantum interference device (SQUID) experiment[12] a Josephson current can be observed in the Kondo regime, when the Kondo temperature T_K is large compared to the superconducting gap Δ, confirming theoretical predictions[14–19] and previous experiments[7,20] (with no determination of supercurrents though).

In the present work we explore in detail this competition between Josephson and Kondo physics by monitoring on the same device as a function of the gate voltage the bias dependence of the differential conductance in the normal state and the Josephson current in the superconducting state. The value of this current is precisely determined by fitting the data with a theoretical model explicitly including the effect of the electromagnetic environment onto the junction. From the normal state data, we extract the charging energy U and the Kondo temperature T_K as a function of the gate voltage and calculate the sum of the couplings to the electrodes $\Gamma=\Gamma_L+\Gamma_R$ from the known form of T_K.[21] The asymmetry Γ_R/Γ_L is determined from the value of the conductance on the Kondo resonance for $T \ll T_K$. The value of this current is precisely determined by fitting the data with a theoretical model explicitly including the effect of the dissipative electromagnetic environment onto the junction. As expected a supercurrent is observed (for an odd number of electrons on the nanotube) when $T_K > \Delta$ and when the asymmetry of the transmission of the electrodes is not too large.[14–19] On the other hand, when $T_K < \Delta$, the magnetic spin remains unscreened at all temperatures leading to a π junction with a very low transmission of Cooper pairs.[22] We have particularly explored in this Rapid Communication the intermediate regime where the Kondo temperature can be tuned with the gate voltage, on a single Kondo ridge, from a value slightly below the superconducting gap at half filling to a value $T_K > \Delta$. A sharp increase in the supercurrent is then observed, which is related to the transition from a magnetic doublet state to a nonmagnetic singlet state of the nanotube island. We compare these results with functional renormalization group (FRG) calculations for the single impurity Anderson model[19] in a wide region of gate voltage.

We grow SWCNTs by chemical vapor deposition on thermally oxidized, highly doped silicon wafers. Individual

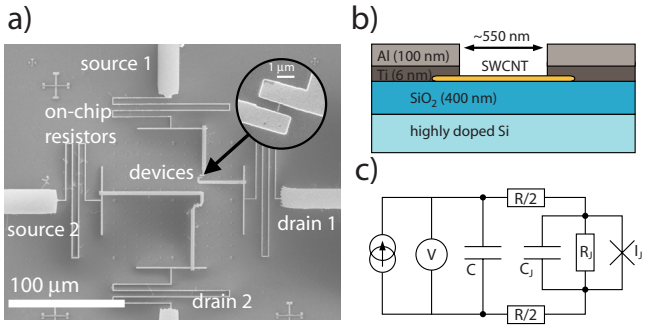

FIG. 1. (Color online) (a) Scanning electron micrograph of the electrical on-chip environment of the nanotube. (b) Cross section of the nanotube with electrodes and backgate (c) Schematic of the carbon nanotube Josephson junction with its environment according to the extended RCSJ model.

SWCNTs are located relative to predefined markers and contacted to Ti/Al leads using electron-beam lithography [Figs. 1(a) and 1(b)]. The Ti/Al leads are superconducting below 1 K. Measurements were done in a dilution refrigerator with a base temperature of $T=40$ mK. The cryostat was equipped with a three-stage filtering system consisting of LC filters at room temperature, resistive microcoax cables, and finally microceramic capacitors in a shielded metallic box, which also contained the samples and was tightly screwed onto the cold finger. As additional filters against voltage fluctuations, resistors of the order of 2 kΩ were implemented on chip as meanders in the Au lines connecting the superconducting electrodes to the contact pads [Fig. 1(a)]. Measurements were done with a lock-in technique with either an ac voltage of 5–10 μV, measuring differential conductance dI/dV, or an ac current of 10 pA, measuring differential resistance dV/dI, both as a function of an additional dc-bias voltage or current, respectively. Figure 1(c) shows a schematic view of our device. It consists of a Josephson junction with current $I_J(\phi)$ parallel to a capacitor C_J and a shunt resistance R_J. We obtain a rough estimate of $C_J \approx 100$ aF from the charging energy $U=e^2/2C_J$. The junction resistor R_J represents the contribution of quasiparticles to dissipation at frequencies of the order of the plasma frequency of the junction ω_P. The outer capacitance C represents the capacitances of the leads to ground within the electromagnetic horizon of the junction, which we estimate as $2\pi c/\omega_p$ to some centimeters, depending on R_J. It is therefore mainly determined by the capacitance of the metallic leads to the highly doped backgate and can be estimated to $C \approx 8$ pF.[23] The series resistances R represent the lithographically defined on-chip resistors. This situation corresponds to the "extended resistively and capacitively shunted junction" (extended RCSJ) model,[10,13,24,25] which we will use later.

We first characterize the CNT quantum dot with the electrodes driven normal by a small magnetic field (100 mT). The color scale plot of dI/dV as a function of $V_{\rm bias}$ and $V_{\rm BG}$ (the "charge stability diagram") displays a regular sequence of "Coulomb blockade diamonds" over a wide range of $V_{\rm BG}$. In other regions this pattern is replaced by a smoother gate dependence characteristic of Fabry-Perot oscillations.[1] For further analysis, we concentrate on the gate voltage region

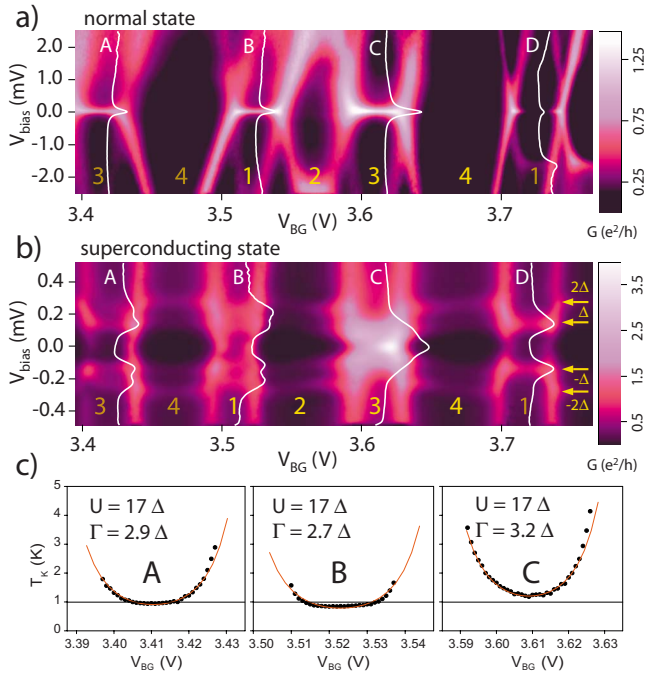

FIG. 2. (Color online) Color scale plot showing gate and voltage bias dependence of the differential conductance. (a) Normal state. (b) Superconducting state. White lines correspond to vertical sections of G versus $V_{\rm bias}$ in the middle of the four Kondo ridges labeled A–D. (c) Gate dependence of the Kondo temperature extracted on the Kondo ridges far from the degeneracy points. The red lines are fits to Eq. (1); the black line corresponds to $T_C=1.0$ K. U and Γ are given in units of Δ.

between 3 and 4 Volts [see Fig. 2(a)]. It shows a fourfold periodicity in the size of the Coulomb blockade diamonds,[26] which indicates a clean nanotube with the twofold orbital degeneracy of the electronic states preserved. We extract $U=2.5\pm0.3$ meV as estimated from the size of Coulomb blockade diamonds with an odd number of electrons. In all states with odd occupation, the Kondo effect manifests itself through a high conductance region around zero bias, the so-called Kondo ridge. The Kondo temperature T_K can be estimated from the half width of the peaks of these lines which can be fitted by Lorentzian curves.[27] The Kondo temperature goes through a minimum on the order of 1 K in the center of the ridges and increases on the edges. It is possible to follow this gate dependence along the Kondo ridges A–C [Fig. 2(c)]. The intensity on ridge D is too weak for such an analysis. T_K can be well fitted by the expression predicted by the Bethe Ansatz,[21]

$$T_K = \sqrt{U\Gamma/2}\,\exp\left[-\frac{\pi}{8U\Gamma}|4\epsilon^2 - U^2|\right], \qquad (1)$$

where ϵ is the energy shift measured from the center of the Kondo ridge. Taking $U=2.5$ meV as determined above, the value of T_K at $\epsilon=0$ leads to the characteristic coupling energies $\Gamma=\Gamma_R+\Gamma_L$ between the electrodes for each Kondo ridge [Fig. 2(c)]. The gate voltage $V_{\rm BG}$ dependence of T_K yields the ratio α between the electrostatic energy $eV_{\rm BG}$ and the Fermi energy of the nanotube ϵ equal to 20 ± 1. This value agrees

to within 20% with the value deduced from the normal state conductance data. This fit based on the single level Anderson impurity model is only valid when U/Γ is sufficiently large and $|\epsilon| \ll U$. Since for all peaks $T \ll T_K$, the maximum conductance of the ridges yields the asymmetry of the coupling Γ_R/Γ_L, 6.8, 6.2, 2.5, and 70 for A–D, respectively.

By switching off the magnetic field, we allow the leads to become superconducting. Figure 2(b) shows dI/dV for the same gate voltage range as in Fig. 2(a) but for a smaller bias voltage range. The BCS-type density of states in the electrodes leads to new features in the stability diagram, which are horizontal lines at $V_{\text{bias}} = \pm 2\Delta_0$ and $\pm\Delta_0$ due to the onset of quasiparticle tunneling and Andreev reflection, respectively. We can derive the value of the superconducting gap $\Delta_0 = 0.15 \pm 0.02$ meV, which corresponds well to the expected $T_C \simeq 1$ K for the bilayer Ti/Al. Although they have similar Kondo temperatures in the normal state, the Kondo ridges, A–D, show a very different behavior when the electrodes are superconducting. The Kondo ridges (A, B, and D) are suppressed or reduced in amplitude by superconductivity, reflecting that $T_K < T_C$ in the center of the Kondo ridge. Contrary to ridges A, B, and D that show a minimum at zero bias, there is a strong enhancement of conductance in ridge C, with G reaching a value roughly four times larger than in the normal state. Note that states A, C, and D show an enhancement of conductance at $V_{\text{bias}} = \Delta/e$ to values larger than the conductance at $V_{\text{bias}} = 2\Delta/e$. This enhancement of the first Andreev process is due to the "even-odd" effect in Andreev transport, which has recently been described in Refs. 9 and 28.

For a measurement of the supercurrent the device has to be current biased. We simultaneously use ac and dc bias while measuring the resulting voltage drop across it. From the ac part, we obtain data on the differential resistance [Fig. 3(a)]. By numerical integration we get I-V curves that show a supercurrent branch and a smooth transition to a resistive branch with higher resistance [Fig. 3(b)]. The transition between the two regimes is not hysteretic, and the supercurrent part exhibits a nonzero resistance R_S at low bias even if we subtract the contribution of the on-chip resistances R. This behavior is common in mesoscopic Josephson junctions that have a high normal state resistance on the order of the resistance quantum h/e^2. To extract the supercurrent, we use a theory that explicitly includes the effect of the dissipative electromagnetic environment onto the junction in the frame of the already mentioned extended RCSJ model.[10,13,24] Using the external resistor R (Ref. 29) [Fig. 1(c)] and temperature T as input parameters, we can thus extract the critical current I_c and the junction resistance R_J, for every measured backgate voltage, from a fit to

$$I(V_{\text{bias}}) = \left\{ I_c \,\text{Im}\left[\frac{I_{1-i\eta}(I_c\hbar/2ek_BT)}{I_{-i\eta}(I_c\hbar/2ek_BT)} \right] + \frac{V_{\text{bias}}}{R_j} \right\} \frac{R_j}{R_j + R}, \quad (2)$$

where $\eta = \hbar V_{\text{bias}}/2eRk_BT$ and $I_\alpha(x)$ is the modified Bessel function of complex order α.[13] The resulting values are plotted as a function of V_{BG} in Figs. 3(c) and 3(d). The junction conductance $G_J = 1/R_J$ relates well to the differential conductance $G_S = 1/R_S$ extracted from the ac part of the current biased data, especially around the resonance degeneracy

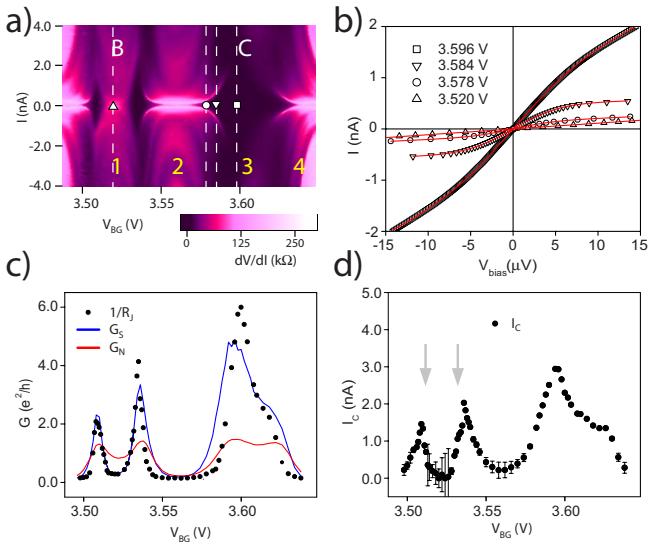

FIG. 3. (Color online) (a) Color scale plot of the differential resistance as a function of dc-bias current and backgate voltage. (b) I-V characteristics for different backgate voltages. The red/gray lines are fits using Eq. (2). (c) Conductances $G_J = 1/R_J$ (black circles), G_S (blue/dark gray line), and G_N (red/gray line). (d) Gate voltage dependence of the critical current extracted from fits to Eq. (2).

points where the conductance is high. The normal state conductance G_N deviates from G_S most notably in states B and C, where Kondo physics plays a key role. In state B, $G_N > G_S$, whereas the ridge in state C persists in the superconducting state, resulting in a further enhancement of the conductance.

The supercurrent exhibits peaks at the maximum values of the conductance [Fig. 3(d)]. Its behavior between peaks varies strongly in states with even and odd occupations. In the following we focus on Kondo ridges B and C. Whereas the supercurrent on ridge C varies nearly proportionally to the conductance, we observe a sharp drop of supercurrent on ridge B as illustrated in Fig. 3(d) (arrows). This can be understood considering that T_K is smaller on ridge B than on ridge C [see Fig. 2(c)]. As a result the magnetic moment of the excess electron on the nanotube remains unscreened in the superconducting state near $\epsilon = 0$ which is not the case for ridge C. At this stage we compare our experimental findings to approximate zero-temperature FRG calculations which allow for extracting both the stability regions of the screened singlet and magnetic unscreened doublet phases and the complete supercurrent-phase relation $I_J(\phi)$ within a model of an Anderson impurity coupled to two superconducting electrodes.[19] It was previously observed that the Josephson current cannot be simply described as a single function of the ratio T_K/Δ.[14] The relevant parameters are the on site Coulomb repulsion energy U, the level position ϵ related to V_{BG}, and the transmission of the electrodes Γ_R and Γ_L compared to the superconducting gap. In Fig. 4 we present a comparison between our experimental data to the theoretical predictions for I_c [defined as the maximum value of $|I_J(\phi)|$ over ϕ], as a function of the position in energy of the Anderson impurity level, for similar values of theoretical and experimental pa-

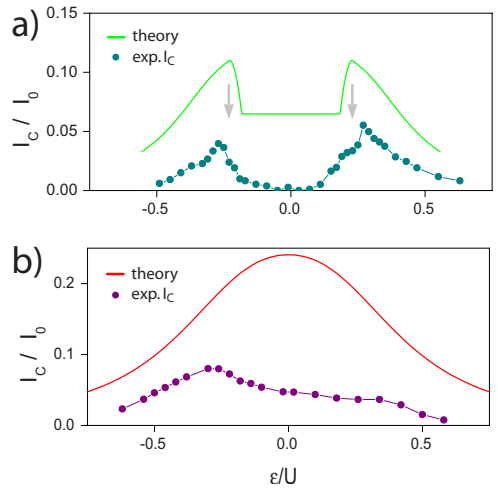

FIG. 4. (Color online) Comparison with FRG calculations: calculated $I_c(\epsilon)$ in units of $I_0=e\Delta/\hbar$ for $\Gamma=2\Delta$, $\Gamma/U=0.11$, $\Gamma_R/\Gamma_L=6$ in (a) and $\Gamma=2\Delta$, $\Gamma/U=0.2$, $\Gamma_R/\Gamma_L=3$ in (b). Experimental data for $I_c(\epsilon)$ are shown for Kondo ridge B in (a) and Kondo ridge C in (b).

rameters. It is remarkable that the gate dependence of the critical current on the Kondo ridges can be qualitatively described, that is, in particular, the existence of a singlet, doublet $(0/\pi)$ transition on ridge B at nearly the right value of gate voltage when renormalized with the charging energy U (arrows) and the absence of a $(0/\pi)$ transition for ridge C corresponding to higher values of T_K. One point of disagreement between theory and experiment concerns the amplitude of the critical current in the doublet state (π junction) region (around $V_{BG}=3.65$ V). I_c is theoretically found to be reduced by only a factor of 2 compared to its value in the singlet region, whereas basically no trace of superconductivity could be detected experimentally. It is known, however, that the π-phase current computed from the approximate FRG is too large compared to numerical renormalization group (NRG) data, which are known to be more accurate but only available at the center of the Kondo ridge.[19]

Finally, let us emphasize the importance of the asymmetry of the transmission of the electrodes which tends to reduce considerably the supercurrent. This is particularly striking for the data on ridge D for which $\Gamma_R/\Gamma_L=70$, where no supercurrent could be measured in spite a value of T_K on the order of 1 K. This reduction of I_c by the asymmetry of contacts is also found in FRG calculations.[19] It is moreover accompanied by a modification of the stability regions for the singlet (screened) and doublet (magnetic) states which strongly depend on the phase difference between the superconducting electrodes. The nonmagnetic singlet state is stabilized with respect to the magnetic doublet state in the vicinity of $\phi=\pi$, which results in a strong modification of the current phase relation which unfortunately cannot be checked in a single I_c measurement.[19]

In conclusion, we have shown that it is possible to tune the amplitude of the supercurrent in a carbon nanotube Josephson junction within a Kondo ridge in a very narrow range of gate voltage. Our data are in good qualitative agreement with theoretical findings and should stimulate new experiments where the whole current phase relation is measured.[30]

We acknowledge fruitful discussions with Y. Avishai, S. Guéron, W. Belzig, A. Levy-Yeyati, T. Novotný, J. Paaske, and B. Röthlisberger. This work was supported by the EU-STREP program HYSWITCH and by the Deutsche Forschungsgemeinschaft via FOR 723 (C.K. and V.M.).

[1] W. Liang *et al.*, Nature (London) **411**, 665 (2001).
[2] B. Babić and C. Schönenberger, Phys. Rev. B **70**, 195408 (2004).
[3] D. Goldhaber-Gordon *et al.*, Nature (London) **391**, 156 (1998).
[4] A. Y. Kasumov *et al.*, Science **284**, 1508 (1999).
[5] A. Kasumov *et al.*, Phys. Rev. B **68**, 214521 (2003).
[6] A. F. Morpurgo *et al.*, Science **286**, 263 (1999).
[7] M. R. Buitelaar *et al.*, Phys. Rev. Lett. **89**, 256801 (2002); M. R. Buitelaar *et al.*, *ibid.* **91**, 057005 (2003).
[8] H. I. Jorgensen *et al.*, Phys. Rev. Lett. **96**, 207003 (2006).
[9] A. Eichler *et al.*, Phys. Rev. Lett. **99**, 126602 (2007).
[10] P. Jarillo-Herrero *et al.*, Nature (London) **439**, 953 (2006).
[11] Tunable supercurrents through Carbon nanotubes have also been observed in T. Tsuneta *et al.*, Phys. Rev. Lett. **98**, 087002 (2007); Y. Zhang *et al.*, Nano Research **1**, 145 (2008); E. Pallecchi *et al.*, Appl. Phys. Lett. **93**, 072501 (2008); G. Liu *et al.*, Phys. Rev. Lett. **102**, 016803 (2009).
[12] J.-P. Cleuziou *et al.*, Nat. Nanotechnol. **1**, 53 (2006); Note that similar devices were made with semiconducting nanowires in J. A. van Dam *et al.*, Nature (London) **442**, 667 (2006).
[13] I. Jorgensen *et al.*, Nano Lett. **7**, 2441 (2007).
[14] L. I. Glazman and K. A. Matveev, JETP Lett. **49**, 659 (1989).
[15] A. V. Rozhkov and D. P. Arovas, Phys. Rev. Lett. **82**, 2788 (1999).
[16] M. S. Choi *et al.*, Phys. Rev. B **70**, 020502(R) (2004).
[17] E. Vecino *et al.*, Phys. Rev. B **68**, 035105 (2003).
[18] F. Siano and R. Egger, Phys. Rev. Lett. **93**, 047002 (2004).
[19] C. Karrasch *et al.*, Phys. Rev. B **77**, 024517 (2008).
[20] K. Grove-Rasmussen *et al.*, N. J. Phys. **9**, 124 (2007).
[21] A. M. Tsvelick and P. B. Wiegmann, Adv. Phys. **32**, 453 (1983); N. E. Bickers, Rev. Mod. Phys. **59**, 845 (1987).
[22] H. Shiba and T. Soda, Prog. Theor. Phys. **41**, 25 (1969); J. Zittartz and E. Müller-Hartmann, Z. Phys. **232**, 11 (1970).
[23] Due to this large value of C it is possible that the finite resistivity of the backgate also contributes to dissipation at very high frequency.
[24] V. Ambegaokar and B. I. Halperin, Phys. Rev. Lett. **22**, 1364 (1969).
[25] M. Tinkham, *Introduction to Superconductivity* (McGraw-Hill, New York, 1996).
[26] M. R. Buitelaar *et al.*, Phys. Rev. Lett. **88**, 156801 (2002).
[27] D. Goldhaber-Gordon *et al.*, Phys. Rev. Lett. **81**, 5225 (1998); Sara M. Cronenwett *et al.*, Science **281**, 540 (1998).
[28] T. Sand-Jespersen *et al.*, Phys. Rev. Lett. **99**, 126603 (2007).
[29] Note the absence of explicit dependence on the capacitances C and C_j for an overdamped junction, as it is the case in our experiment ($Q=0.03$).
[30] M. L. Della Rocca *et al.*, Phys. Rev. Lett. **99**, 127005 (2007).